An Improved High-Power Factor and Low-Cost Three-Phase Rectifier

Ewaldo L. M. Mehl, *Student Member, IEEE* and Ivo Barbi, *Senior Member, IEEE*

***Abstract*—A new method to improve the power factor of three-phase rectifiers is introduced in this paper. The main features of the proposed circuit are low cost, small size, high efficiency, and simplicity. The power factor improvement is achieved with three bi-directional active switches rated at a small fraction of the total processed power, and gated at the line frequency. The principle of operation and design procedure, with a practical example, are also presented. The theoretical analysis was validated with experimental results from a laboratory prototype rated at 7.4 kW and connected to the 220-V 60-Hz ac system. The same circuit was also used in another prototype rated at 12 kW, with similar results.**

***Index Terms*— AC–DC converter, power factor, three-phase rectifier.**

I. Introduction

IN THE recent years, a number of new techniques have been proposed for improving the power factor of three-phase rectifiers. Prasad *et al.* introduced in [1] a dc–dc boost topology with a three-phase rectifier and three boost inductors at the ac side. Although the circuit draws a high-quality current from the ac source, with almost unity power factor, in high-power application the boost switch stands as a challenging design problem. Other proposals utilize special magnetic devices to achieve a high-power factor without active switches, as the circuit presented by Kim *et al.* [2], or use line interphase transformers [3]–[5]. In such cases, the cost, volume, weight, and additional power losses on the magnetic components withstand as a major limitation for high-power applications. On the other hand, the circuit proposed in [6] and shown in Fig. 1(a) makes use of three low-power bidirectional switches, each gated on at the line frequency at the instant when the input ac voltage crosses zero. The circuit features low cost, simplicity, and high efficiency and is particularly appropriate for high-power application. However, that converter requires a connection to the neutral wire of the ac system, and due to that connection a pulsed current is present on the neutral. It was also noticed in the circuit of Fig. 1(a) that the energy stored at the input inductors is responsible for building up high voltage stresses across the switches during the turn-off commutation.

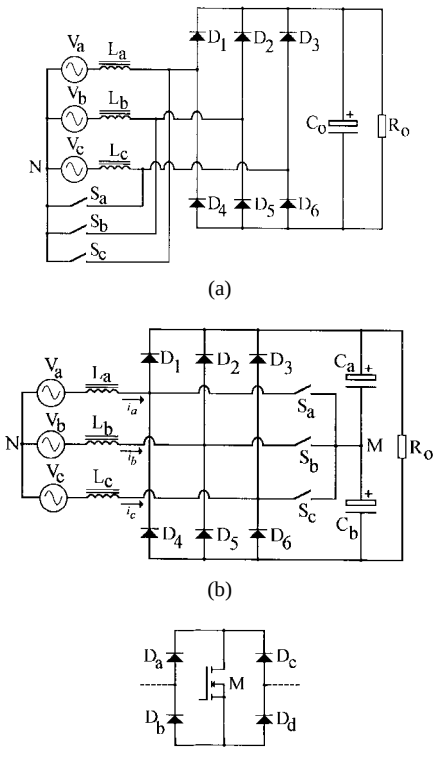

Fig. 1. (a) Circuit presented in [6]. (b) Improved high-power-factor three-phase rectifier. (c) Bidirectional switch used in the prototype.

Although these voltage stresses can be limited with clamping circuits, circuit reliability is reduced and losses are increased.

In order to overcome those drawbacks, in this paper an improved ac-to-dc converter is introduced and validated by laboratory prototypes. The power circuit is pictured in Fig. 1(b) and, albeit possessing all the attributes of the one presented in [6], does not require a connection to the neutral wire, operates with lower input current, shows lower harmonic distortion, and does not need any clamping circuit to prevent excessive overvoltage across the active switches during the turn-off commutation.

II. Circuit Description and Analysis

The voltage sources V_a, V_b, and V_c in Fig. 1 denote the three-phase ac system. Diodes D_1 to D_6 are low-frequency rectifiers, with load R_o and input inductors L_a, L_b, and L_c. The filter capacitor C_o in Fig. 1(a) was replaced by two identical capacitors C_a, and C_b in Fig. 1(b), in order to accomplish a balanced central node between the positive

Paper IPCSD 96–52, approved by the IEEE Industrial Applications Society for presentation at the 1996 IEEE Power Electronics Specialist Conference, Lake Maggiore, Italy, June 24–27, and the 1995 Applied Power and Electronics Conference and Exposition, Dallas, TX, March 5–9.

E. L. M. Mehl is with the Department of Electrical Engineering, Federal University of Paraná, Curitiba, PR 81531-970, Brazil.

I. Barbi is with the Federal University of Santa Catarina, Power Electronics Institute, Florianópolis, SC 88040-970, Brazil.

Publisher Item Identifier S 0093-9994(97)01537-5.

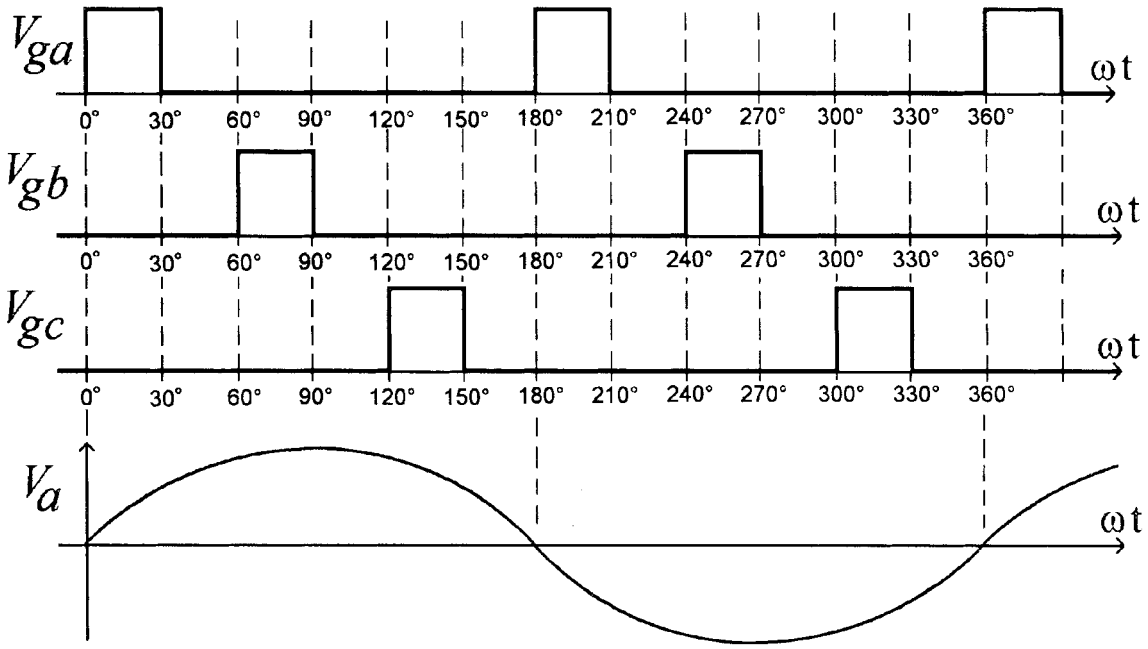

Fig. 2. The low-frequency switching pattern presented in [6].

and negative output terminals. In the prototypes, each of the bidirectional switches S_a, S_b, and S_c were assembled with a low-power MOSFET connected between the dc nodes of a diode bridge, as in Fig. 1(c). The resulting power circuit is similar to the high-frequency PWM rectifier presented in [7]; however, in the proposed converter, the switches operate at low frequency and the gating circuit is a very simple one.

Fig. 2 shows the gate scheme for the bidirectional switches on the proposed converter. In a conventional three-phase diode rectifier with capacitive load, the line current shows a delay of approximately 30° relative to the line voltage, resulting in periodical intervals where such current is null. The effect is a low power factor and high harmonic distortion of the input current. On the proposed rectifier, each of the bidirectional switches S_a, S_b, and S_c is gated on during an appropriate interval, providing an alternative path for the input current. Each gate pulse starts when the corresponding phase voltage is null, with a pulse width denoted by α. On a first approach, α was set to 1/12 of the voltage period, or 30°, for all the load conditions of the converter. Using a suchlike switching pattern, the bidirectional switches operate at low frequency, with reduced power losses, and use low-cost devices. Along with this feature, the input inductors can be assembled with ordinary core materials, resulting in a low-cost ac-to-dc converter with a high power factor, suitable to high-power applications.

For the circuit analysis, in Fig. 3, six topological stages are presented, corresponding to the 0°–180° half-period shown in Fig. 2; for simplicity, only the components where current is present were pictured at each of those intervals.

Two main situations can be identified in Fig. 3.

1) In the stages (a), (c), and (e), there are only two conducting diodes. As a result, on a conventional three-phase rectifier, the current on the third phase remains null during that interval. In the proposed circuit, the switch associated with the third phase is gated on during that interval. For instance, during the 0°–30° stage in Fig. 3(a), the switch S_a is gated on, so the input current i_a evolves from zero to a maximum value ruled by (1), where L is the input inductance of the inductors L_a, L_b, and L_c, and V_i is the rms input line voltage:

$$i_a(t) = \frac{\sqrt{2} \cdot V_i}{2 \cdot \pi \cdot f \cdot L\sqrt{3}} (1 - \cos \omega t). \tag{1}$$

From (1), a simple equivalent circuit for the input current i_a can be derived, shown in Fig. 4 and valid for the 0°–30° stage. The same equivalent circuit can be used for modeling the input current associated with phase "B" when S_b is gated on (60°–90°) and for phase "C" when S_c is gated on (120°–150°). As a result, the voltage across the points M and N [Fig. 1(b)] is null for the stages (a), (c), and (e) in Fig. 3.

2) In the stages (b), (d), and (f), there are three conducting diodes, one associated with each phase. The three switches are off, so the converter behaves like a conventional rectifier with input inductors. As a result, the circuit analysis produces differential equations similar to (2) for each phase:

$$\frac{d}{dt} i_a(t - t_o) = \frac{V_a(t - t_o)}{L} - \frac{V_o}{3 \cdot L}. \tag{2}$$

The differential equations can be solved using Laplace transformation and employing the value of the input current at the end of each stage as the initial value on the next stage. This procedure leads to a set of equations describing the input current in each phase as a function of the dc output voltage (V_o). For instance, during the 150°–180°interval, the input

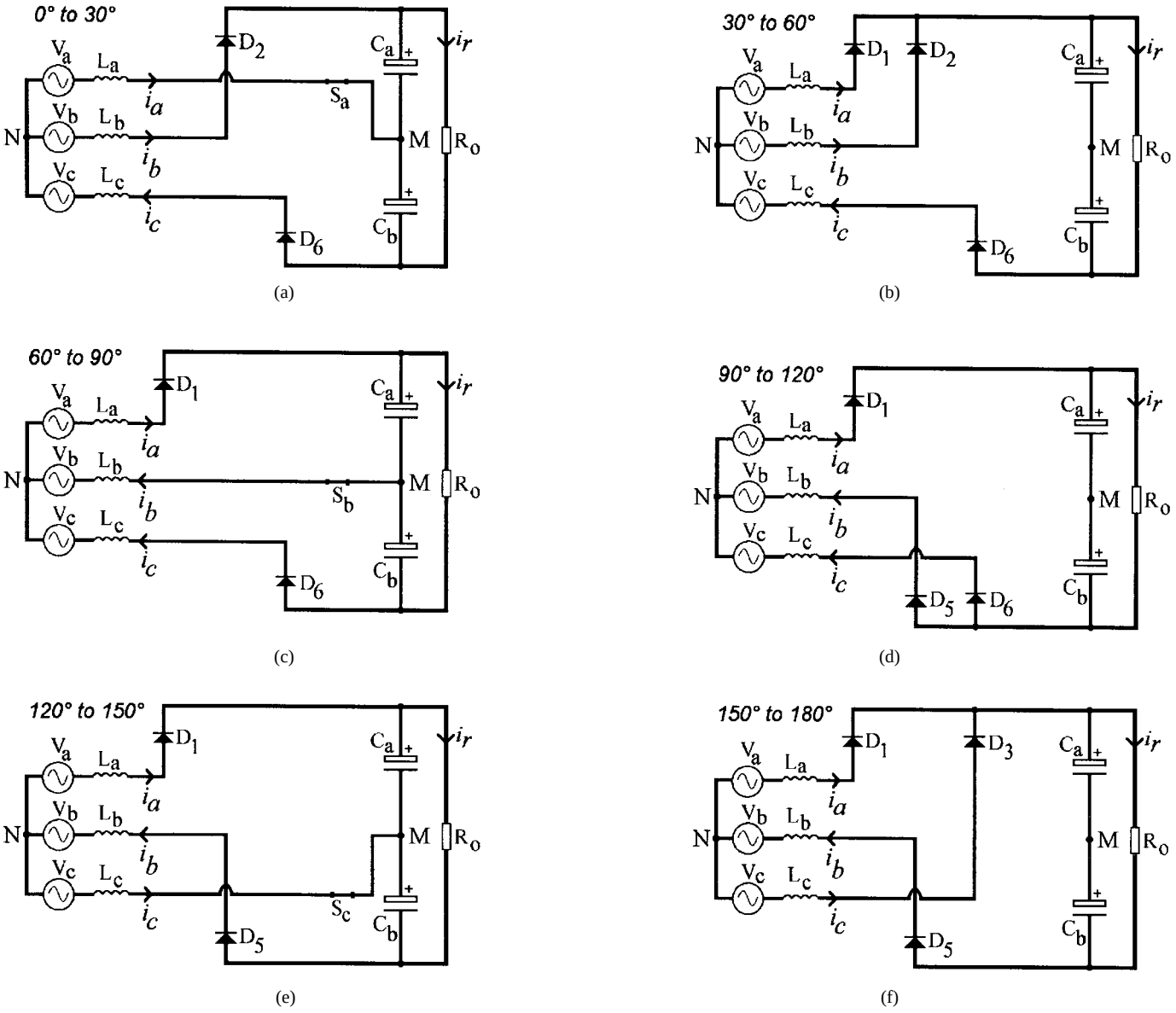

Fig. 3. Topological stages for a half-period of the V_a input voltage.

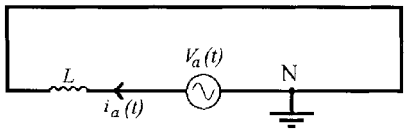

Fig. 4. Equivalent circuit for i_a (phase "A" input current) during the 0°–3° stage, when the switch S_a is gated on.

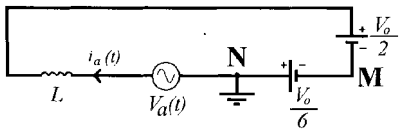

Fig. 5. Equivalent circuit for i_a (phase "A" input current) during the 30°–60° stage.

current on phase "A" is ruled by (3):

$$i_a(t) = \frac{\sqrt{2}\cdot V_i}{3\cdot\omega\cdot L}\left[\sqrt{3}\sin(\omega\cdot t) + 3\cos(\omega\cdot t) - 3\right] - \frac{V_o}{3\cdot L} + \frac{3\sqrt{2}\cdot V_i + 2\sqrt{3}\sqrt{2}\cdot V_i - 2\pi\cdot V_o}{6\cdot\omega\cdot L}. \quad (3)$$

Similar expressions as (3) can be written for phase "B" and "C" and for the other stages when the switches are off. As a result, equivalent circuits can be derived, as that one shown in Fig. 5 for the 30°–60° stage. In that equivalent circuit, two dc voltage sources can be noticed, one $(V_o/2)$ for modeling the C_a output capacitor and the other one $(V_o/6)$ for the voltage across the points M and N.

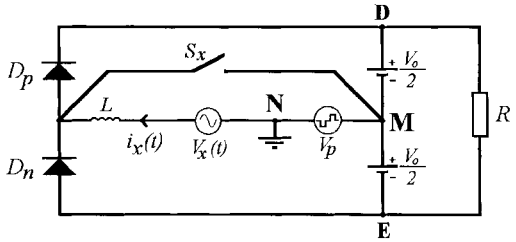

Fig. 6. Simplified equivalent circuit for the circuit analysis.

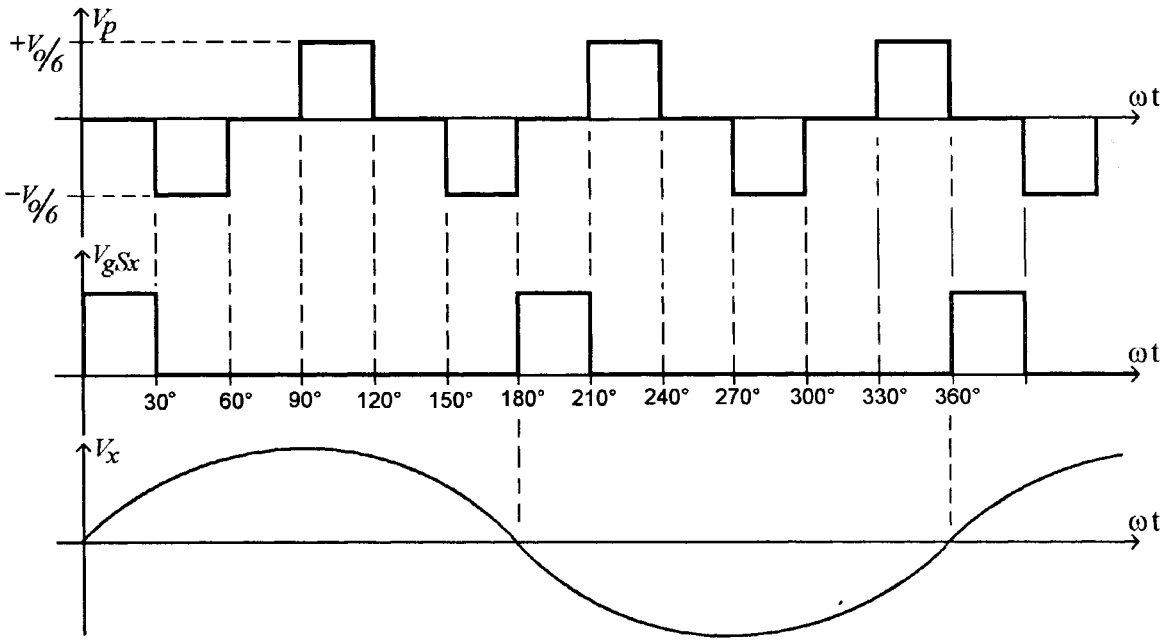

Fig. 7. Voltage pattern of the V_p pulsed source and the V_x sinusoidal source, along with the switching pattern for the S_x switch, for the simplified equivalent circuit shown in Fig. 6.

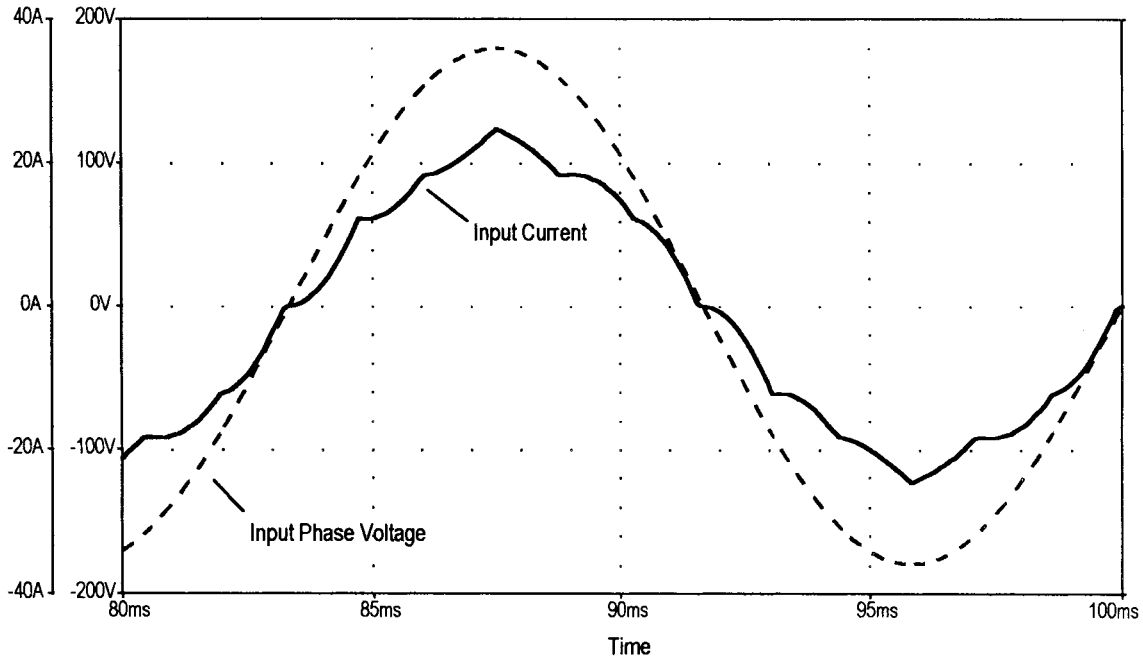

Fig. 8. PSpice circuit simulation of the input current and corresponding input phase voltage.

With the partial equivalent circuits of Figs. 4 and 5, a general equivalent circuit can be inferred as seen in Fig. 6. The voltage of the central point M, using the node N as the reference, can be modeled by a three-level pulsed voltage source V_p as represented in Fig. 7.

There is a particular value to the L inductance in the equivalent circuit that can be considered as the "critical inductance" of the circuit. With such value of inductance, at 180° and 360° the input current i_x reaches zero, concomitant with the V_x voltage zero-volt transition. Therefore, assuming that (3) is null for $\omega \cdot t = 180°$, the dc output voltage of the converter is calculated with (4):

$$V_o = \left(\frac{36 \cdot \sqrt{2}}{7 \cdot \pi \cdot \sqrt{3}}\right) V_i = 1.3366 \cdot V_i. \tag{4}$$

The "critical inductance" can be calculated with (5), assuming that the input current feeds the load during the 90°–120° interval of Fig. 3(d):

$$L = \frac{36}{7}\left(2\sqrt{3} - 3\right) \cdot \frac{(V_i)^2}{2 \cdot \pi^3 \cdot f \cdot P_o} = 3.8489 \times 10^{-2} \cdot \frac{(V_i)^2}{f \cdot P_o}. \tag{5}$$

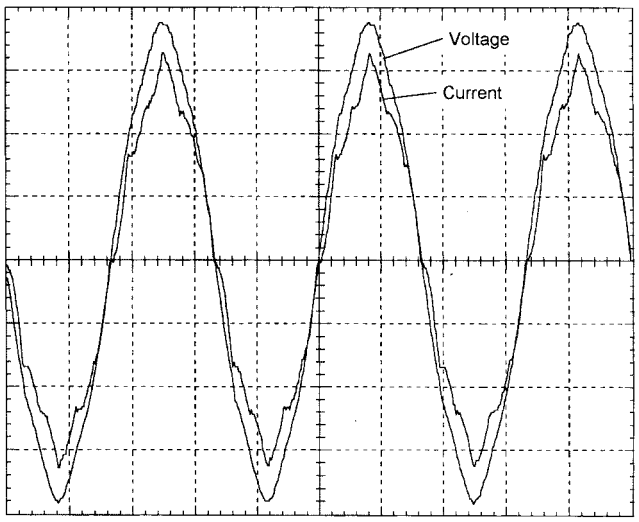

Fig. 9. Input current and voltage for 7.4-kW power output. Scales: voltage = 50 V/div; current = 10 A/div; and time = 5 ms/div.

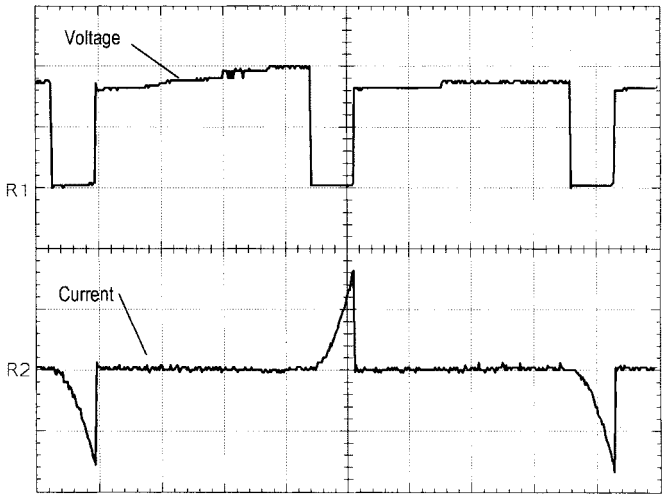

Fig. 10. Drain-source voltage on the MOSFET and external current of S_a for $\alpha = 30°$. Scales: voltage = 100 V/div; current = 10 A/div; and time = 2 ms/div.

As illustrated in Fig. 2, the current flows trough the bidirectional switches just during the 0°–30° and 180°–210° intervals. Making $\omega \cdot t = 30°$ in (1), the peak current trough one switch is given by (6):

$$I_{sw(\max)} = 1.7410 \times 10^{-2} \cdot \frac{V_i}{f \cdot P_o}. \tag{6}$$

For the 30°–180° and 210°–360° periods, the switch is off. As a result, the rms value of the switch's current is given by (7) and the average current is calculated with (8):

$$I_{sw(\mathrm{rms})} = 2.2624 \times 10^{-3} \cdot \frac{V_i}{f \cdot P_o} \tag{7}$$

$$I_{sw(\mathrm{avg})} = 4.8807 \times 10^{-4} \cdot \frac{V_i}{f \cdot P_o}. \tag{8}$$

Meanwhile, the voltage across the switch's terminals is lower than half of the output voltage when the switch is off.

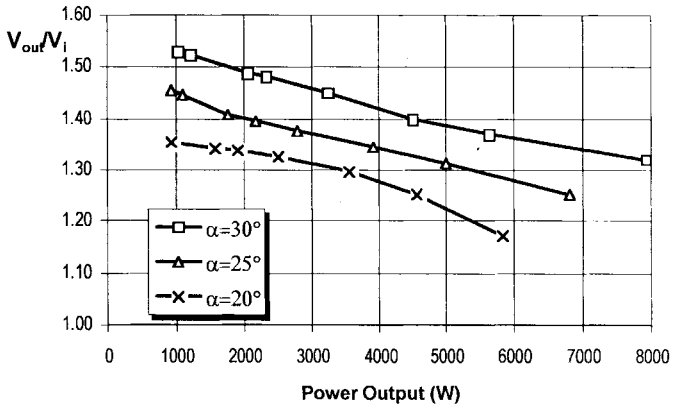

Fig. 11. Output characteristics of the 7.4-kW prototype.

III. Design Example and Simulation

In order to illustrate the design procedure, a converter with the following specifications is assumed:

- ac line input voltage (across phases): $V_i = 220$ V;
- ac frequency: $f = 60$ Hz;
- Output power: $P_o = 7.4$ kW.

The "critical inductance" is calculated with (5), giving:

$$\begin{aligned} L &= 3.8489 \times 10^{-2} \cdot \frac{(V_i)^2}{f \cdot P_o} \\ &= 3.8489 \times 10^{-2} \cdot \frac{(220)^2}{60 \times 7400} \\ &= 4.19 \text{ mH}. \end{aligned}$$

The dc output voltage for the nominal power output is calculated with (4) and results:

$$\begin{aligned} V_o &= 1.3366 \cdot V_i \\ &= 1.3366 \times 220 \\ &= 294.1 \text{ V}. \end{aligned}$$

The circuit as seen in Fig. 1(b) was simulated using PSpice. Fig. 8 shows the input current though one of the input inductors with the corresponding input phase voltage. Also with PSpice, the Fourier analysis gives a total harmonic distortion (THD) of 6.3% for the input current, resulting to a power factor of 0.998.

IV. Experimental Results

With the previously simulated results, a first laboratory prototype was assembled to validate the proposed technique, using the same specifications as the simulation example.

From (6), the peak current through each bidirectional switch is 15.96 A. However, the rms value of such current is 2.07 A and the average current is just 0.45 A. The maximum voltage across each switch is about 150 V. Therefore, low-power components can be used for the switch's assembly. Each of the bidirectional switches, S_a, S_b, and S_c, was therefore assembled as in Fig. 1(c) with a IRF740 MOSFET (M) connected between the dc nodes of a rectifier bridge, made up with four SK3G/04 Semikron diodes (D_a, D_b, D_c, and D_d). The main rectifier diodes [D_1 to D_6 in Fig. 1(b)] are Semikron SKN12/12. The input inductors L_a, L_b, and L_c were

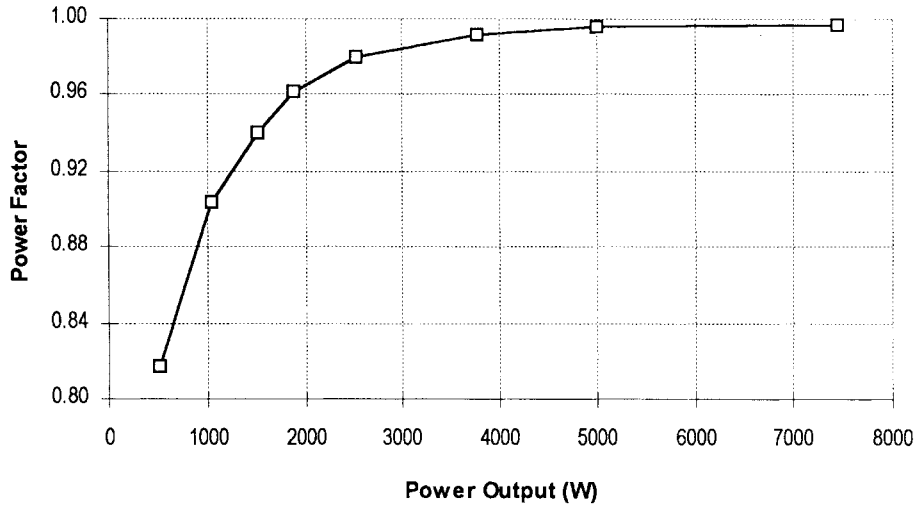

Fig. 12. Power factor of the 7.4-kW prototype, measured at several load conditions and constant 291.5-V output voltage.

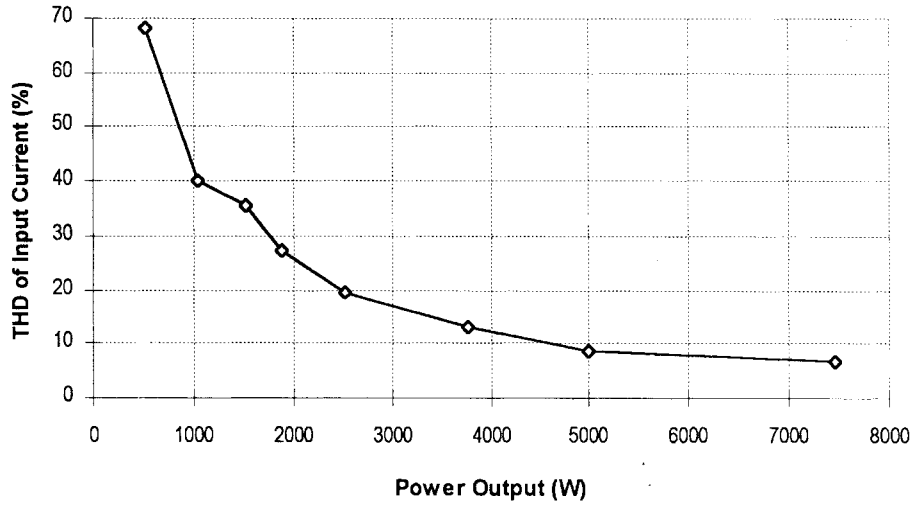

Fig. 13. THD on the input current of the 7.4-kW prototype, measured at several load conditions and 291.5-V output voltage.

constructed with ordinary silicon-steel E-I sheets, with an air gap to provide inductance adjustment. Each of the inductors weighed about 2.9 kg (6.4 lb). A very simple open-loop control circuit was arranged in order to adjust simultaneously the conduction angle (α) of the three switches from 0° to 30°.

By the point of view of the proposed converter, the capacitance of the output capacitors C_a and C_b is not critical. They must withstand, however, the current pulses produced by the switches' operation. In industrial applications, the high output current of the converter will naturally require special grade capacitors that will easily tolerate the additional switching pulses. For the 7.4-kW prototype, two 600-μF $\times$ 250-V capacitors where used for C_a and C_b.

Bench tests of the prototype were conducted with an assortment of high-power wire resistors connected as the load. At 7.45-kW load condition, the measured output voltage was 291.5 V and the waveforms of the resulting input current and of the phase voltage are shown in Fig. 9. The Fourier analysis of the input current issues a THD of 6.56% and the resulting power factor is 0.996. For 7.43-kW dc output power, the measured ac input power was 7.66 kW, resulting in an efficiency of 97%.

In contrast to the topology proposed in [6], no overvoltage stresses are presented on the switches. Fig. 10 shows the drain-source voltage across the MOSFET and the current that flows through one of the bidirectional switches, for $\alpha = 30°$. Since each MOSFET conducts current just for a short interval, the rms value of that current is very low, and power loss is minimal.

Fig. 11 shows the output characteristic of the 7.4-kW prototype. It is evident that the conduction angle α can be used to control the output voltage over an extended power output range. To verify the ability of the proposed rectifier to achieve a high power factor with a constant output voltage, the dc output voltage of 291.5 V obtained at the 7.43-kW load condition was chosen as the goal value. On the following tests, for each load condition the conduction angle α was adjusted manually in order to have 291.5 V for the output voltage.

The results of the bench tests with constant output voltage are presented in Figs. 12 and 13. It is observed that the

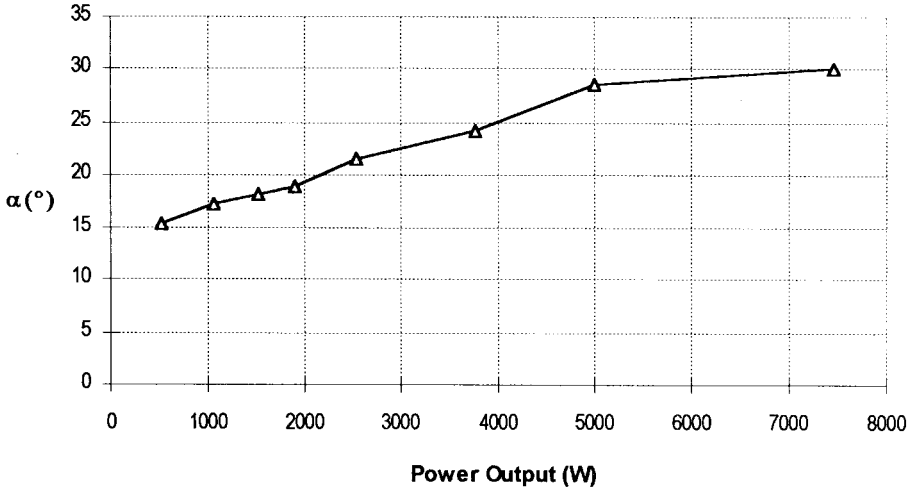

Fig. 14. Adjustments made on the conduction angle (α) of the switches S_a, S_b, and S_c, on the 7.4-kW prototype, in order to obtain output voltage of 291.5 V.

prototype can achieve a high power factor over an extended output power range, with regulated output voltage. Fig. 14 shows the variation of the conduction angle α, between 15° for 500-W output power and 30° for 7.43-kW output power.

It can be noticed in Figs. 12 and 13 that both the power factor and THD are degraded in low-output power region, because the "critical inductance" is calculated for the nominal load condition. However, the power factor is still grater than 0.98 and the THD is lower than 10% for the 4–7.4-kW range. Some proposals for extending that range were extensively discussed in [8]. A novel switching proposal for the same circuit, for extending the output power range with low THD, can also be found in [9].

After the promising results achieved with the 7.4-kW prototype, another converter was built, rated at 12 kW, with the same topology [Fig. 1(b)] and connected to the three-phase 220-V/127-V ac supply. The "critical inductance" for that output power value is 2.58 mH and is calculated with (5). Although the output power of the converter is quite high, the rms current on the switches is 4.51 A and average current is just 1.38 A. The main components used in the second prototype were:

- input inductors: $L_a = L_b = L_c = 2.6$ mH;
- output capacitors: $C_a = C_b = 2250\,\mu$F;
- diodes: $D_1 = D_2 = D_3$ =Semikron SKN26/04; $D_4 = D_5 = D_6 =$ Semikron SKR26/04;
- MOSFET's for S_a, S_b, and S_c: APT6040BN;
- diodes for S_a, S_b, and S_c: Semikron SK3G10.

In the same procedure used for the first prototype, the capacitors for C_a and C_b were chosen with their current characteristic and not by the capacitance.

For preliminary tests, the same gate pulse generator circuit used for the 7.4-kW prototype was used. The new prototype showed a similar behavior of the previously presented one. At 11.9-kW power output, with conduction angle $\alpha = 30°$, the output voltage was 296.1 V. The THD of the input current was 10.5% for that load condition, with main input waveforms shown in Fig. 15.

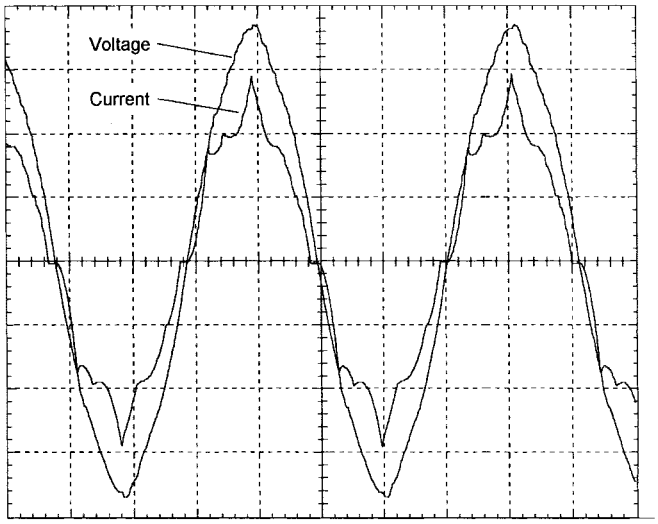

Fig. 15. Experimental input current and phase voltage for the second prototype at 11.94-kW output power. Scales: voltage = 50 V/div; current = 20 A/div; and time = 4 ms/div.

Although the THD is higher (10.5%) than the one achieved with the first prototype (6.56%), the resulting power factor of the 12-kW prototype is 0.994.

V. Conclusion

This paper presents a new ac-to-dc high-power factor three-phase diode rectifier with three low-power bidirectional switches gated at low frequency. The proposed technique can be used to build new high-power rectifiers and can be added to existing apparatus, since the main rectifier diodes are little affected by the presence of the bidirectional switches. Two laboratory prototypes rated 7.4 and 12 kW were evaluated through bench tests.

Although very similar to the topology presented in [6], the new converter shows some remarkable advantages.

- No connection is needed to the ac system neutral wire. As a result, the third harmonic component is automatically eliminated.

- The power factor of [6] was increased and is almost unitary at the nominal load condition.
- The turn-off overvoltage presented on the circuit of [6] was also eliminated in the proposed topology.
- For the same values of the conduction angle α, the new converter showed a higher output voltage characteristic, which could be convenient for switch-mode power supply applications.

Other important features of the proposed rectifier are the following.

- A high power factor is achieved over an extended output power range.
- The rated power of each auxiliary switch is very low in contrast to the high output power of the rectifier. Therefore, the switches can be assembled with low-cost semiconductor devices and power losses are minimal.
- As the auxiliary switches operate at low frequency, the gating circuit is elementary and there is no necessity of fast-switching semiconductor devices.
- The turn-off voltage stresses across the semiconductor devices are low. No clamping circuits are necessary.
- The input inductors operate at low frequency and were assembled using ordinary silicon-steel material for the cores. Although it is necessary to have inductance on the range of several milihenrys, the high magnetic flux density of the metal leads to small inductors. The cost of the low-frequency core material is also insignificant in contrast to the high-frequency ferrite material that would be necessary for building high-frequency inductors.
- The conduction angle of the switches can be adopted as a control variable to perform the output voltage regulation of the rectifier, while keeping the power factor near unity over a significant range of the output power.

REFERENCES

[1] A. R. Prasad, P. D. Ziogas, and S. Manias, "An active power factor correction technique for three-phase diode rectifiers," in *IEEE/PESC Conf. Rec.,* 1989, pp. 58–66.

[2] S. Kim, P. N. Enjeti, P. Packebush, and I. J. Pitel, "A new approach to improve power factor and reduce harmonics in a three-phase diode rectifier type utility interface," *IEEE Trans. Ind. Applicat.,* vol. 30, pp. 15557–1564, Nov./Dec. 1994.

[3] C. Niermann, "New rectifier circuits with low mains pollution and additional low cost inverter for energy recovery," in *EPE Conf. Rec.,* 1989, pp. 1131–1136.

[4] A. F. Souza, D. J. M. Fernandes, N. Bonacorso, and I. Barbi, "A high performance 100 A/48 V rectifier system with power factor correction," in *Second Brazilian Power Elec. Conf. Rec.,* 1993, pp. 183–188.

[5] C. Muñoz, B. Barbi, and I. Barbi, "A new high power factor three-phase diode rectifier," in *IECON Conf. Proc.,* 1995, pp. 451–456.

[6] I. Barbi, J. C. Fagundes, and C. M. T. Cruz, "A low cost high power factor three-phase diode rectifier with capacitive load," in *IEEE APEC Conf. Proc.,* 1994, pp. 745–751.

[7] J. W. Kolar and F. C. Zach, "A novel three-phase, three-switch, three-level unity power factor PWM rectifier," in *28th PCIM Conf.,* Nürnberg, Germany, 1994.

[8] E. L. M. Mehl, "Proposition, analysis, design and practical implementation of a new three-phase rectifier with high power factor," doctoral dissertation, Universidade Federal de Santa Catarina, Brazil, 1996, in Portuguese

[9] F. Daniel, R. Chaffai, and K. Al-Haddad, "Three-phase diode rectifier with low harmonic distortion to feed capacitive loads," in *IEEE APEC Conf. Proc.,* 1996, pp. 932–938.

Ewaldo L. M. Mehl (A'90–S'92) was born in Curitiba, Brazil, in 1956. He received the degree in electrical engineering from the Federal University of Paraná, Curitiba, Brazil, in 1980, the masters degree in materials engineering from the Federal University of Rio de Janeiro, Rio de Janeiro, Brazil, in 1987, and the Doctor in Electrical Engineering degree from the Federal University of Santa Catarina, Brazil, in 1996, working under the supervision of Prof. I. Barbi on high power factor ac-to-dc converters.

He is currently an Associate Professor at the Federal University of Paraná in Curitiba, Brazil, in the Department of Electrical Engineering. He also worked for several years as a Researcher at LAC, an electrical and electronics research center in Curitiba, Brazil, that is sponsored both by the Federal University of Paraná and COPEL, the electrical utility of the state of Paraná. His primary areas of interest are in high-power converters, power factor correction, and circuit simulation.

Ivo Barbi (M'78–M'87–SM'90) was born in Gaspar, Santa Catarina, Brazil, in 1949. He received the B.S. and M.S. degrees in electrical engineering from the Federal University of Santa Catarina, Florianópolis, Brazil, in 1973 and 1976, respectively, and the Doctor of Engineering degree in 1979 from the Institute National Polytechnique of Toulouse, Toulouse, France.

He founded the Power Electronics Institute of the Federal University of Santa Catarina and was the first president of the Brazilian Power Electronics Society. He is currently a Professor at the Power Electronics Institute. Since 1992, he has been Associate Editor in the power converters area of the IEEE TRANSACTIONS ON INDUSTRIAL ELECTRONICS.